AD-A113 859 MASSACHUSETTS INST OF TECH CAMBRIDGE DEPT OF MATERIA--ETC F/G 7/4
AN SCF-X ALPHA-SH MOLECULAR-ORBITAL STUDY OF A POSSIBLE REACTIO--ETC(U)
MAR 82 A C BALAZA, K H JOHNSON N00014-75-C-0970
UNCLASSIFIED TR-15 NL

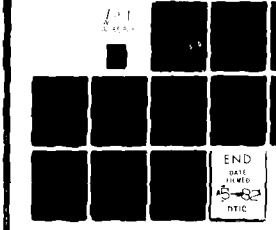

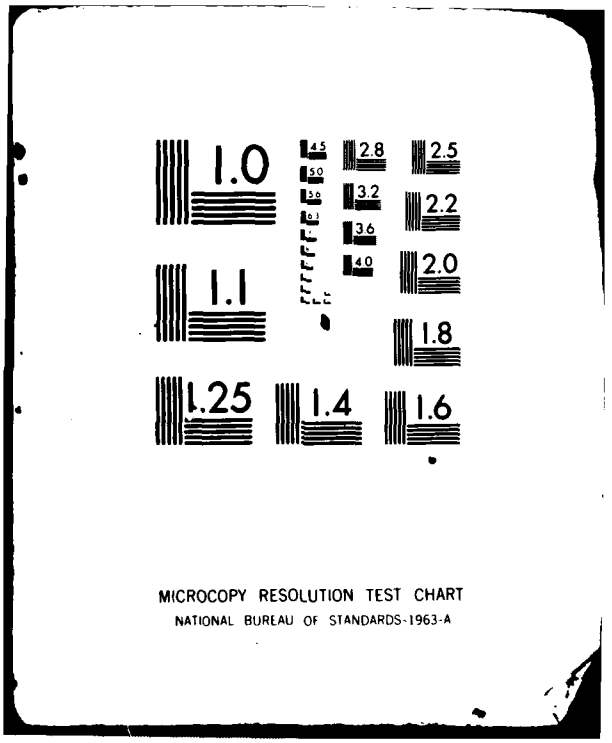
1.0
1.1
1.25
1.4
1.6
1.8
2.0
2.2
2.5
2.8
3.2
3.6
4.0
4.5
5.0
5.6
MICROCOPY RESOLUTION TEST CHART
NATIONAL BUREAU OF STANDARDS-1963-A

Unclassified

SECURITY CLASSIFICATION OF THIS PAGE (When Data Entered)

REPORT DOCUMENTATION PAGE	READ INSTRUCTIONS BEFORE COMPLETING FORM
1. REPORT NUMBER: 15	2. GOVT ACCESSION NO.: AD-A113 559	3. RECIPIENT'S CATALOG NUMBER
4. TITLE (and Subtitle): An SCF-Xα-SW Molecular-Orbital Study of a Possible Reaction Path for Ziegler-Natta Catalysis.	5. TYPE OF REPORT & PERIOD COVERED: Interim
	6. PERFORMING ORG. REPORT NUMBER
7. AUTHOR(s): Anna C. Balazs and Keith H. Johnson	8. CONTRACT OR GRANT NUMBER(s): N00014-75-C-0970
9. PERFORMING ORGANIZATION NAME AND ADDRESS: Department of Materials Science and Engineering, M.I.T., Cambridge, MA 02139	10. PROGRAM ELEMENT, PROJECT, TASK AREA & WORK UNIT NUMBERS: Task No. NR056-596
11. CONTROLLING OFFICE NAME AND ADDRESS: Office of Naval Research, Department of the Navy, Arlington, Virginia 22217	12. REPORT DATE: March 23, 1982
	13. NUMBER OF PAGES
14. MONITORING AGENCY NAME & ADDRESS (if different from Controlling Office)	15. SECURITY CLASS. (of this report): Unclassified
	15a. DECLASSIFICATION/DOWNGRADING SCHEDULE

AD A113559

16. DISTRIBUTION STATEMENT (of this Report)

Approval for public release; distribution unlimited.

17. DISTRIBUTION STATEMENT (of the abstract entered in Block 20, if different from Report)

DTIC ELECTE APR 1 9 1982 S H D

18. SUPPLEMENTARY NOTES

19. KEY WORDS (Continue on reverse side if necessary and identify by block number)

Molecular-Orbital, Study Reaction Path, Ziegler-Natta-Catalysis

alpha

20. ABSTRACT (Continue on reverse side if necessary and identify by block number)

SCF-Xα-SW molecular-orbital calculations for the coordination complex, $[CH_3TiCl_4(C_2H_4)]^{n=0,-2}$, which is postulated to be an intermediate in Ziegler-Natta polymerization reactions, demonstrate that the energy gap between the lower-lying Ti-alkyl orbital and the higher Ti($3d_{yz}$) - olefin(π^*) orbital is sufficiently large (0.9ev for n = 0 and 1.5eV for n = -2) to make the Cossee mechanism for the propagation step seem unlikely, A series of calculations for $CH_3TiCl_4(C_2H_4)$, where the

DD FORM 1 JAN 73 1473 EDITION OF 1 NOV 65 IS OBSOLETE S/N 0102-LF-014-6601

Unclassified 82 04 19 058

SECURITY CLASSIFICATION OF THIS PAGE (When Data Entered)

DTIC FILE COPY

alkyl and olefin groups are moved closer together in a sequence of concerted steps, suggest that this migration is a plausible mechanism for the polymerization reaction.

OFFICE OF NAVAL RESEARCH

Contract N00014-75-C-0970

Task No. NR 056-596

TECHNICAL REPORT NO. 15

AN SCF-Xα-SW MOLECULAR-ORBITAL STUDY OF A POSSIBLE REACTION PATH FOR ZIEGLER-NATTA CATALYSIS

by

Anna C. Balaza and Keith H. Johnson

Department of Materials Science and Engineering

Massachusetts Institute of Technology

Cambridge, Massachusetts 02139

March 23, 1982

ABSTRACT

SCF-Xα-SW molecular-orbital calculations for the coordination complex, $[CH_3TiCl_4(C_2H_4)]^{n=0,-2}$, which is postulated to be an intermediate in Ziegler-Natta polymerization reactions, demonstrate that the energy gap between the lower-lying Ti-alkyl orbital and the higher $Ti(3d_{yz})$ - olefin(π^*) orbital is sufficiently large (0.9eV for n = 0 and 1.5eV for n = -2) to make the Cossee mechanism for the propagation step seem unlikely. A series of calculations for $CH_3TiCl_4(C_2H_4)$, where the alkyl and olefin groups are moved closer together in a sequence of concerted steps, suggests that this migration is a plausible mechanism for the polymerization reaction.

INTRODUCTION

One of the earliest proposals for the mechanism of Ziegler-Natta catalysis was put forth by Cossee,[1] whose qualitative quantum-mechanical treatment was based largely on ligand-field theory. Since then, there has been an increased sophistication in the computational techniques employed in calculating the electronic structure of molecules.[2] Using semiempirical molecular-orbital calculations on Ziegler-Natta type catalysts, investigators [3-7] have recently attempted to verify the postulates of the Cossee mechanism for the polymerization of olefins. The structure of the active site proposed by Cossee (for both the homogeneous and heterogeneous catalysts) was the octahedral complex $RTiCl_4(C_2H_4)$, where R is an alkyl group (Fig. 1).[1] According to this model, when the olefin enters the coordination sphere of the $RTiCl_4$ site, a new, partially occupied molecular orbital is formed through mixing of the metal 3d and ethylene π^* antibonding orbitals. The energy of the new orbital is proposed to be sufficiently below the energy of the original metal 3d levels so that an electron from the Ti-alkyl bonding orbital can easily be thermally excited into it. Consequently, the metal-alkyl bond will be weakened and the alkyl group will be expelled as a radical. The radical attaches intself in a concerted process to the nearest carbon atom of the olefin while at the same time, the other side of the olefin connects itself to the metal. The reaction path is shown in Figure 2.

From more recent molecular-orbital studies of this reaction path, a new explanation has been suggested to account for the polymerization reaction.[3] Here, no radical breaking is necessary to produce polymerization and the Ti d orbitals permit and, in fact, promote the process while the olefin and alkyl groups, still attached to the catalytic site,

migrate towards each other in a series of concerted steps.

Due to the complexity of the reactions involved in Ziegler-Natta catalysis, experimental evidence for the mechnism is far from being complete or unequivocable. For both homogeneous and heterogeneous systems, the complete function of the base metal, e.g., Aℓ, is still debated.[8] Taken collectively, however, the evidence strongly argues that the chain growth reaction occurs at the transition metal ion.[9] Most recently, Evitt and Bergman [10] have established insertion of an olefin into the metal-carbon bond of an intermediate cobalt-alkyl complex as the mechanism for the observed ethylene methylation. This lends credibility to the type of reaction path shown in Figure 2.

In a previous paper,[11] self-consistent field-Xα-scattered wave (SCF-Xα-SW) molecular-orbital claculations[12] were carried out for titanium halide and ethylene-titanium halide complexes as a basis for understanding the bonding of an olefin to clusters relevant to Ziegler-Natta catalysis. The SCF-Xα-SW description of the electronic structure of the titanium trihalides proved to be quite realistic since excitation energies for d-d transitions and charge-transfer transitions were well reproduced. In this paper, we extend the study of Ziegler-Natta catalysis by examining the electronic structure of the coordination complex, $CH_3TiCl_4(C_2H_4)$ (see Fig. 1), which models the active site proposed by Cossee. We have studied the evolution of the electronic structure of the complex in a sequence of six steps whereby the methyl migrates toward the olefin and the olefin inserts into the Ti-methyl bond (Fig. 2). From these studies, we hope to develop some understanding of the propagation steps in Ziegler-Natta polymerization.

Similar models of soluble Ti Ziegler-Natta catalysts have been

examined using the Extended Hückel[6] and CNDO molecular-orbital methods.[3,4(a+b)] The SCF-Xα-SW technique has been shown to have certain advantages over these techniques for the investigation of transition metal complexes.[13] A comparison of our results with those obtained by the methods cited above will be made in the last section of this paper.

STRUCTURAL AND COMPUTATIONAL PARAMETERS

The SCF-Xα-SW energy-level diagram for the most pertinent molecular orbitals along the reaction path (from step a to f) are shown in Figure 3. Step a corresponds to the initial complex shown in Fig. 1, while the molecule described by step f is approaching $TiCl_4(C_3H_7)$. Computational and structural parameters are compiled in Tables I and II (refer to Fig. 1). All constituent atoms, and thus the $CH_3TiCl_4(C_2H_4)$ molecule were taken to be electrically neutral. In the homogeneous catalyst, two of the chlorine ligands are bridging to a base metal ion, while for the heterogeneous system, the four chlorine ligands bridge to two other Ti ions in the lattice.[1] The charge on these bridging chlorines is impossible to predict a priori. Consequently, the neutral species may represent a model that is too oxidized, i.e., it has too few electrons. On the other hand, another system that could be investigated, $[CH_3TiCl_4(C_2H_4)]^{-2}$ will represent a model that is too reduced. For this study, we have chosen to examine the reaction path in Figure 2 using the neutral species. However, we have also examined the electronic structure of the $[CH_3TiCl_4(C_2H_4)]^{-2}$ complex, retaining the geometry shown in Fig. 1. We will comment briefly on this calculation as well.

RESULTS AND DISCUSSION

Though the $CH_3TiC\ell_4(C_2H_4)$ molecule consists of 51 valence electrons which are distributed among 26 orbitals, the titanium-carbon bonding is described by only two orbitals (see Fig. 3a). These then will be the most important orbitals to consider. With respect to the Ti-olefin bond, only the ethylene π orbital ($1b_{3u}$) mixes significantly with the Ti orbitals. Here, Ti exhibits a mixture of 4s (7%), 4p (53%) and $3d_{x^2-y^2}$ (40%) character (see Table III). This molecular orbital corresponds to σ forward-donation bonding in the classic Dewar-Chatt model[14] - the ethylene π orbital contributes to the σ bond by donating charge into empty Ti d orbital. However, the charge in this level is fairly localized on the ethylene moiety, with only 10 percent of the charge residing in the Ti atomic sphere (see Table III). This fact, as well as the rather poor degree of overlap displayed in Fig. 5(a) indicate a relatively weak Ti-ethylene interaction. Weak Ti-ethylene bonding also characterized an earlier SCF-Xα-SW calculation[11] on the "surface complex" $[Ti(C_2H_4)C\ell_5]^{-2}$.

The orbital directly above the Ti-olefin σ-bonding orbital is the highest occupied molecular orbital (Fig. 3a) This orbital displays strong covalent overlap between the carbon p and Ti d_{z^2} orbitals [see Fig. 6(a)]. This orbital also shows some mixing with the ethylene π^* level, but the amount of charge in the carbon spheres of the ethylene molecule (less than 1 percent) makes this interaction insignificant.

The $3d_{yz}$-π^* orbital constitutes the lowest unoccupied molecular orbital (LUMO) of this system. However, almost all the charge (86%) is localized on the Ti atom and the orbital lies only slightly lower in energy (by 0.3eV) than the nearly degenerate d_{xz} and d_{xy} levels. This orbital displays a weak Ti-alkyl antibonding interaction, but, again,

the amount of charge on the alkyl carbon makes this interaction insignificant. Recalling that one of the postulates of the Cossee model[1] is the occupation and enhanced stability of the d_{yz}-π^* orbital, we already see a discrepancy with this model. Moreover, since the HOMO and LUMO are separated by 0.9eV, the probability of thermal excitation from the Ti-alkyl level to the d_{yz}-π^* orbital, proposed by Cossee as the critical step, seems unlikely.

A calculation for the electronic structure of $[CH_3TiCl_4(C_2H_4)]^{-2}$ indicates that the $3d_{yz}$-π^* orbital is now singly occupied, but again 86% of the charge is found on the Ti center with only 4% localized on each carbon atom of ethylene. Such charge polarization indicates that π back-donation or charge flow from the occupied Ti d_{yz} orbital into the empty ethylene π^* orbital is indeed relatively small. The energy gap between this orbital and the now doubly occupied Ti-alkyl orbital is increased to 1.5eV, again alleviating the possibility of thermally induced occupancy of this orbital.

Having characterized the Ti-carbon interaction in the starting complex, we now examine how the quantities discussed above change as the nuclei move. Table III indicates how the charge distribution and Ti hybridization in the pertinent orbitals change as the alkyl and olefin molecules are moved along the reaction path. The approximate atomic charges on the Ti and carbon species in the various positions are given in Table IV. The wavefunction contour maps in figures 5 and 6 display how the original Ti-olefin and Ti-alkyl bonding orbitals corresponding to the occupied energy levels in Fig. 3 evolve along the reaction paths. Fig. 4 locates the positions of the atomic species in the molecular-orbital contour maps (a) for the intial complex in Figs. 5 and 6.

Though all the orbitals play some part in the reaction scheme, it is the changes in the Ti-alkyl and Ti-olefin bonding orbitals that are the most revealing. Frames (b) through (d) of Fig. 6 indicate a most striking effect as the alkyl group migrates towards the C(2) carbon of ethylene. Figure 6(b) shows a weak initially antibonding interaction between C(1) (the alkyl carbon) and C(2) (only 1% of the charge is located in this ethylene carbon at this step, see Table III), while, in Fig. 6(c) and (d), one can see a complete rotation of the C(2) p_y orbital, away from the initial π bond with the other ethylene carbon and towards σ overlap with C(1). A driving force for this motion may be the greater bond strength of p-p σ bonds over p-p π bonds. Consequently, whereas Fig. 6(b) displays the ethylene π orbitals, by frame (d) it is the π^* antibonding orbital that is localized on the ethylene site (which continues to gain charge in further steps). The greater participation of the π^* orbital in this coordination sphere effectively weakens the ethylene π bond.

The weakening of the ethylene π bond can also be seen in Fig. 5(b)-(d). Here, the p_y orbital on the C(2) atom, initially strongly involved in the C(2)-C(3) π bond [frame (a)] tips away from the C(3) atom and towards the C(1) carbon. This motion destabilizes the ethylene π bond and initiates the C(1)-C(2) σ bond. It is clear in frames (e)-(f) of the same figure that the C(2)-C(3) π bond has now been broken and that the carbon atoms are connected through a chain of σ bonds. While the charge has clearly localized on C(2) and C(3) in the initial frame, it is essentially delocalized among all three carbon centers in frame (f) (see Table III). Also notable in Fig. 5 is a continuous decrease in the degree of Ti-olefin bonding. Consequently, the Ti($d_{x^2-y^2}$)-ethylene (π)

σ bond in Fig. 5(a) gives way to a carbon-carbon bonding orbital for the C_3H_7 molecule in Fig. 5(f).

Concomitant with the ethylene π bond breaking, a weakening of the Ti-alkyl bond is also seen in frames (b)-(d) of Fig. 6. This can be noted, for example, by observing that the highest value contour lines defining the Ti d lobe and the C(1) p lobe no longer overlap in frames (c) and (d) as they did in frames (a) and (b). It should also be noted in Fig. 6 that the Ti d_{z^2} orbital which had previously been directed toward the alkyl atom in frame (a) now evolves into a d_{yz} orbital. Frames (b) and (c) highlight yet another important interaction: as the Ti-C(1) bond strength decreases, the overlap between a lobe of the metal d_{yz} and C(3) increases, as does the charge in the C(3) center. (This is again a d-p σ-type bond).

Examination of these molecular orbitals suggests that the activation barrier for this reaction should occur along the steps outlined in frames (b) through (d). This observation is in qualitative agreement with total-energy calculations performed by Novaro, et al.,[4(b)] who found that the activation barrier for the reaction path in Figure 2 coincides with the ethylene π-bond breaking steps. In an intermediate state [Figure. 6(d)], the formation of a tricenter bond between the Ti d_{yz},C(1) and C(2) indicates the charge is free to flow in the region between the substituents. Consequently, there is no further barrier to the migration of the alkyl group towards the olefin [see Fig. 5(e)-(f)].

The experimentally observed low activation energy (8-12 kcal/mole) for this process (both homogeneous[15] and heterogeneous[16]) may be explained in this model by the following: (1) C-C π bonds are broken in favor of

the formation of the stronger C-C σ bonds, (2) Ti-C(1) bond breaking is accompanied by Ti-C(3) bond formation and (3) there are no additional barriers to the proposed migration.

Figure 6(f) reflects a dramatic rearrangement in the electronic structure of the complex relative to that shown in Fig. 6(a) for the initial configuration. At this point in the reaction path, the Ti-alkyl distance has been increased to 2.61Å and all C-C bond lengths are practically equal (see Table II). The bonding between Ti and C(3) increases in going from step (a) to (f) (see Table IV), as the metal tips toward C(3) for more complete overlap in the formation of a strong sigma bond. This interaction helps secure one end of the growing polymer chain to the metal center. The Ti-C(3) bonding orbital, which also displays strong C(1) and C(2) bonding [see Fig. 6(f)], now lies well below the HOMO and is doubly occupied [see Fig. 3(f)]. This then constitutes the Ti-propyl bonding orbital. As can be seen, the site previously occupied by the alkyl group is now vacant. Examination of a low-lying unoccupied Ti(d_{z^2}) antibonding orbital of the resulting Ti-propyl complex (Fig. 7) reveals that this site is capable of accepting electrons from and forming a σ bond with the π orbital of an incoming ethylene molecule and consequently the polymerization reaction can be repeated. It would appear that migration of the propyl chain back to the initial Ti-alkyl bonding site, proposed by Cossee as the last step in the reaction path, does not seem to be a mandatory step for continued chain growth.

It is possible that an electrostatic attraction between the negatively charged methyl carbon, C(1), and a positively charged ethylene carbon, C(2), may either initiate [3] or drive the reaction to completion. From Table V we see that the electrostatic attraction between C(1) and C(2)

would potentially be largest in steps (d) to (f). Although the net positive charge is greater on the Ti than on C(2), at step (d) C(1) is closer to C(2) than Ti and consequently, this electrostatic attraction may drive the reaction to completion.

Summary

Experimental ambiguity prevents one from modeling a well characterized active site. However, the present model does provide an accurate description of how the Ti orbitals are perturbed in the presence of the alkyl and olefin groups. These results disagree with Cossee's prediction[1] of a strong interaction between the Ti $3d_{yz}$ and the ethylene π^* orbitals. Moreover, the large energy difference between the Ti-alkyl and $3d_{yz}$-π^* orbitals in the $[CH_3TiCl_4(C_2H_4)]^{n=0,-2}$ complexes makes the Cossee mechanism for polymerization seem extremely unlikely. Instead, the present results are in excellent qualitative agreement with the predictions (based on semiempirical molecular orbital calculations on soluble catalyst systems) made by Armstrong, et al.[3] and Novaro, et al.[4] Specifically, both investigators find that the Ti-methyl bond is localized in the HOMO, where the Ti d orbital makes a large contribution to the bond. Though Armstrong and Novaro disagree as to the extent of $3d_{yz}$-π^* interaction, both find that this orbital constitutes the LUMO. Both authors propose that there is no need to consider initial labilization of the metal-carbon bond by thermal excitation but rather that the reaction between the alkyl and the olefin can proceed through a concerted motion of these moieties. Though our computational procedures do not allow for a reliable calculation of the total energy, which thus precludes an estimate of the activation energy, we find this mechanism to be symmetry allowed along each step of the hypothesized reaction path. Moreover, examination of the SCF-$X\alpha$-SW

molecular-orbital wavefunctions suggest that while C-C π bonds are being broken, C-C σ bonds are being made and that the loss in Ti-C(1) d-p σ bonding. These observations lead us to conclude that the above mechanism is consistent with the experimentally observed low activation energy for Ziegler-Natta catalysis.

ACKNOWLEDGMENTS

This work was supported by the Office of Naval Research and, in part, by the National Science Foundation (DMR-78-24185).

REFERENCES

1. P. Cossee, J. Catal. 3, 80 (1964).
2. See, for example, Semiempirical Methods of Electronic Structure Calculation, Part A; Techniques, edited by G. A. Segal (Plenum, New York, 1977).
3. D. R. Armstrong, P. G. Perkins and J. J. Stewart, J. Chem. Soc., Dalton Trans. 1972 (1972).
4. (a) G. Giunchi, E. Clementi, J. E. Ruiz-Vizcaya, and O. Novaro, Chem. Phys. Lett. 49, 8 (1977);
   (b) O. Novaro, El Blisten-Barojas, E. Clement, G. Guinchi and M. E. Ruiz-Vizcaya, J. Chem. Phys. 68, 2337 (1978);
   (c) O. Novaro, S. Chow and P. Maynouat, J. Catal. 41, 91 (1976).
5. J. W. Begley and F. Pennella, J. Catal. 8, 203 (1967).
6. P. Cossee, P. Ros and J. H. Schachtschneider, Proceedings of the Fourth International Congress on Catalysis, Moscow, 1968, (Academiai Kiado, Budapest, 1971), p. 237.
7. R. J. McKinney, J. Chem. Soc. Chem. Comm. 11, 490 (1980).
8. E. G. M. Tornqvist, Ann. N.Y. Acad. Sci. 155, 447 (1969).
9. J. Boor, Jr., Ziegler-Natta Catalysts and Polymerizations, (Academic Press, New York, 1979), p. 361.
10. E. R. Evitt and R. G. Bergman, J. Amer. Chem. Soc. 101, 3973 (1979).
11. N. Rösch and K. H. Johnson, J. Mol. Catal. 1, 395 (1976).
12. (a) J. C. Slater and K. H. Johnson, Phys. Rev., B5, 844 (1972);
   (b) K. H. Johnson and F. C. Smith, Jr., Phys. Rev., B5, 831 (1972)
   (c) K. H. Johnson, in, Advances in Quantum Chemistry, Vol. 7, edited by P. O. Löwdin (Academic Press, New York, 1973), p. 143.
13. R. P. Messmer, S. K. Knudson, K. H. Johnson, J. B. Diamond, and C.Y. Yang, Phys. Rev., B13, 1396 (1976).

REFERENCES

14. (a) M. J. S. Dewar, Bull. Soc. Chim. Fr., 18, C79 (1951);

    (b) J. Chatt and L. A. Duncanson, J. Chem. Soc. 2929 (1953).

15. J. C. W. Chien, J. Amer. Chem. Soc. 81, 86 (1959).

16. G. Natta and I. Pasquon, Adv. Catal. 11, 1 (1959).

Table I

Exchange parameters, α, and sphere radii, r, (a.u.) used in the SCF-Xα-SW calculations of $CH_3TiCl_4(C_2H_4)$.

	α[a]	r
Outer Sphere	0.73720	7.4395[b]
Ti	0.71695	2.5543
C	0.75331	1.7827
H	0.77725	1.2500
Cl	0.72325	2.7572

(a) These values were taken from Ref. 11.

(b) This value was increased in further steps to accommodate the increasing distance between the Ti and migrating alkyl group.

Table II

Structural Parameters[a]

Step	$Ti-C_1=r_1$ (Å)	$Ti-C_3=r_2$ (Å)	$C_2-C_3=r_3$ (Å)	θ (degrees)	ϕ (degrees)
a	2.10[b]	2.22[c]	1.34[d]	0.0	0.0
b	2.17	2.22	1.35	14.5	8.9
c	2.32	2.16	1.38	25.1	14.9
d	2.43	2.13	1.47	30.2	24.9
e	2.56	2.12	1.54	34.8	30.0
f	2.61	2.12	1.54	36.4	30.0

(a) The Ti-Cl distance is held constant at 2.45 Å, Ref. 11.

(b) Ref. 7.

(c) Ref. 11.

(d) H. Allen, Jr. and E. K. Plyler, J. Am. Chem. Soc. 80, 2673 (1958).

Table III

The titanium and carbon charge distribution for the orbitals in Figure 5, as well as the partial wave decomposition for the metal center

Step	Ti	s	p	d	C(1)	C(2)	C(3)
a	10	7	53	41	1	23	20
b	11	10	44	46	11	21	15
c	5	4	67	29	9	13	9
d	3	3	75	22	7	7	6
e	5	0	46	54	9	5	6
f	4	0	44	56	10	5	6

Table IV

The titanium and carbon charge distribution for the orbitals in Figure 6, as well as the partial wave decomposition for the metal center

Step	Ti	S	p	d	C(1)	C(2)	C(3)
a	32	6	20	75	33	0	1
b	47	1	6	93	18	1	10
c	60	0	3	97	12	0	12
d	60	0	3	97	11	1	12
e	54	0	4	96	9	4	14
f	50	0	4	96	10	5	15

Table V

Atomic charges on the titanium and carbon atoms along the reaction path

Step	Ti	C(1)	C(2)	C(3)
a	+0.87	+0.03	+0.07	+0.09
b	+0.88	+0.04	+0.12	+0.09
c	+0.90	+0.01	+0.14	+0.10
d	+0.91	-0.04	+0.24	+0.13
e	+0.92	-0.14	+0.19	+0.12
f	+1.02	-0.19	+0.14	+0.11

FIGURE CAPTIONS

Figure 1. The coordinate system and geometry of the initial $CH_3TiCl_4(C_2H_4)$ complex, as well as the parameters which are varied in the calculations.

Figure 2. A schematic diagram for the reaction path proposed by Cossee. R is the alkyl group, V is the vacant site and X is a halid ion.

Figure 3. The SCF-Xα-SW energy level diagram for the relevant orbitals along the reaction path.

Figure 4. Positions of the atomic species in the initial $CH_3TiCl_4(C_2H_4)$ complex.

Figure 5. Contour plots for the evolution of the Ti-olefin molecular-orbital wavefunction stages of the reaction path (the lowest occupied orbital in Fig. 3). The contour values are ±0.003, ±0.009, ±0.027 and ±0.081. See Fig. 4 for the positions of the atoms in the initial complex (a).

Figure 6. Contour plots for the evolution of the Ti-alkyl molecular-orbital wavefunction stages of the reaction path (the HOMO in Fig. 3). The contour values are ±0.003, ±0.009, ±0.027 and ±).081. See Fig. 4 for the positions of the atoms in the initial complex (a).

Figure 7. Contour plot for the LUMO wavefunction of the product $TiCl_4(C_3H_7)$ complex. The contour values are ±0.003, ±0.009, ±0.027 and ±0.081.

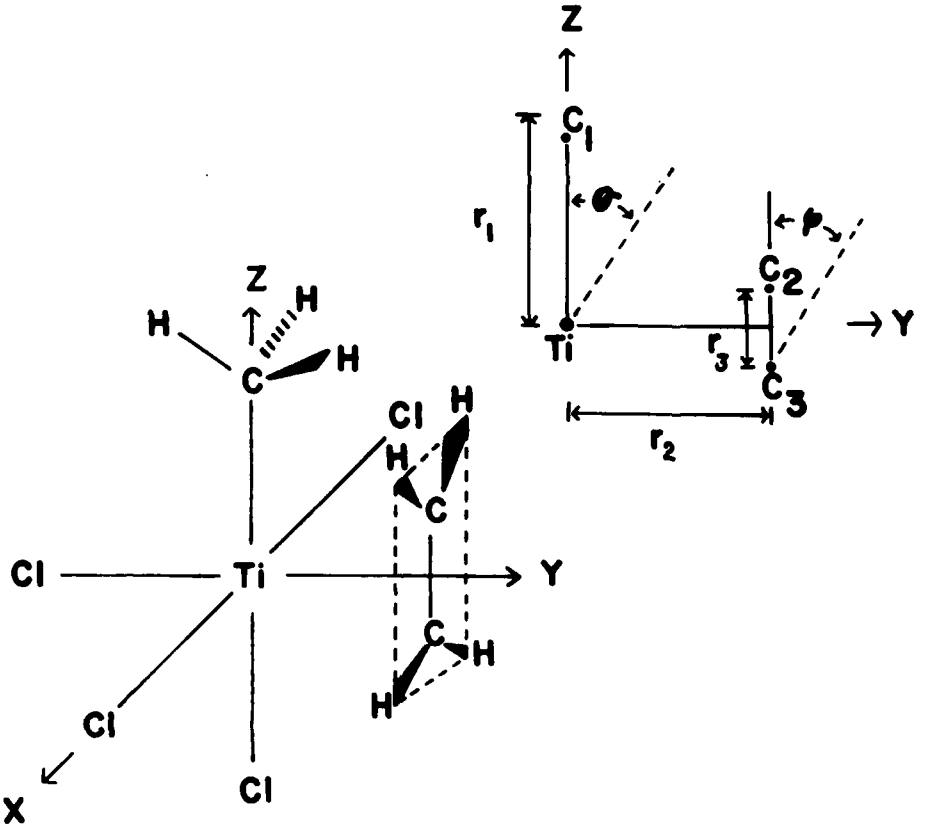
Z
H
H
C
H
Cl
H
H
C
Cl
Ti
Y
C
H
H
Cl
X
Cl
Z
C1
r1
C2
Y
Ti
r3
C3
r2

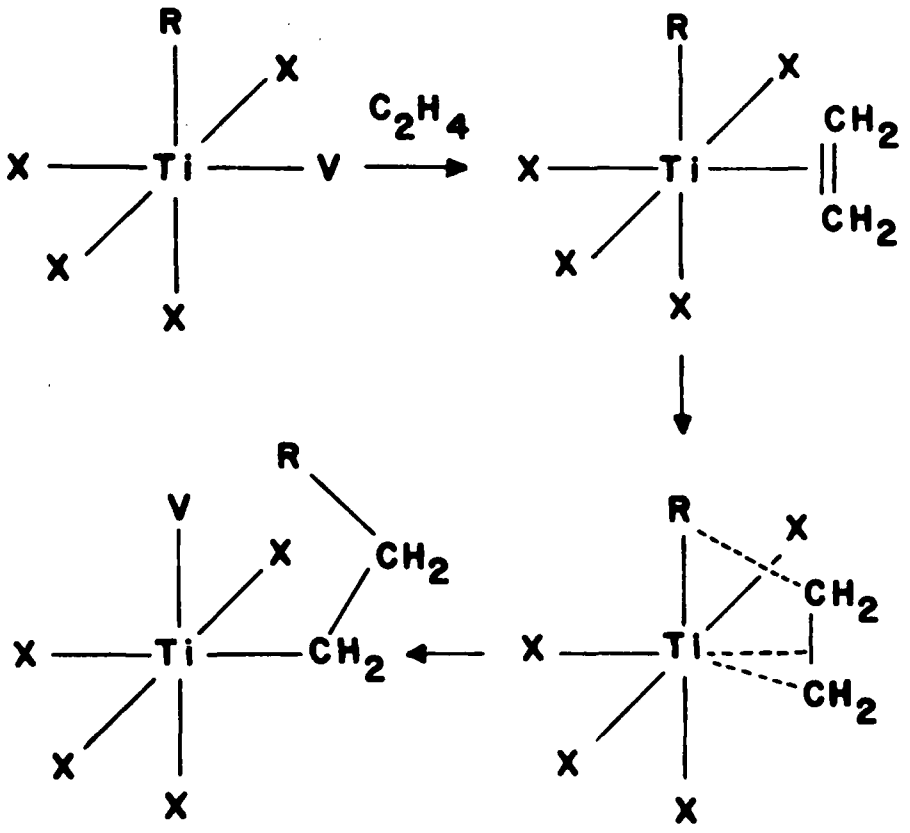
R
X
X
Ti
V
X
X
C_2H_4
R
X
CH_2
X
Ti
CH_2
X
X
R
X
CH_2
X
Ti
CH_2
X
X
R
V
X
CH_2
X
Ti
CH_2
X
X

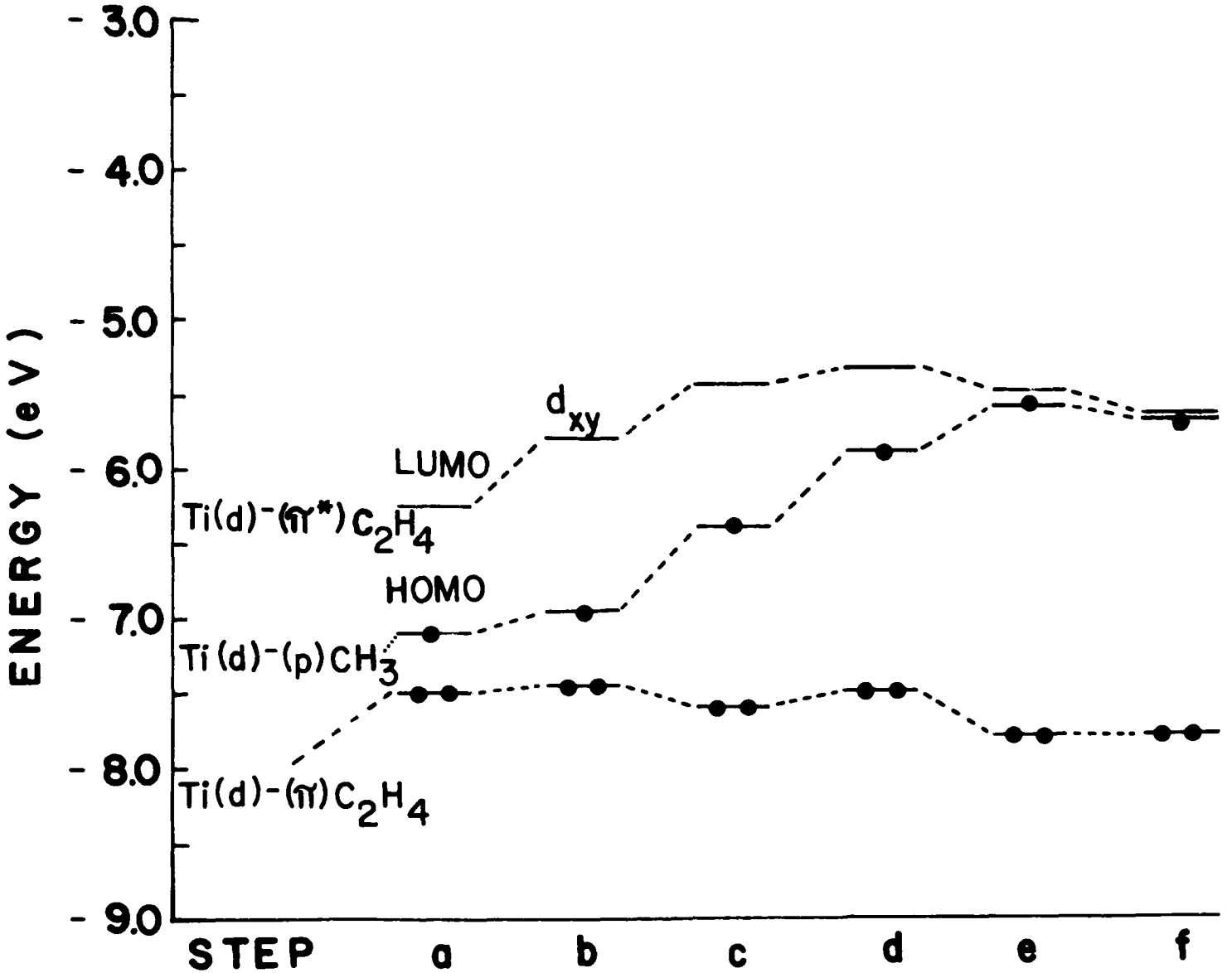
- 3.0
- 4.0
- 5.0
- 6.0
- 7.0
- 8.0
- 9.0
ENERGY (eV)
d_{xy}
LUMO
Ti(d)-(π^*)C_2H_4
HOMO
Ti(d)-(p)CH_3
Ti(d)-(π)C_2H_4
STEP
a
b
c
d
e
f

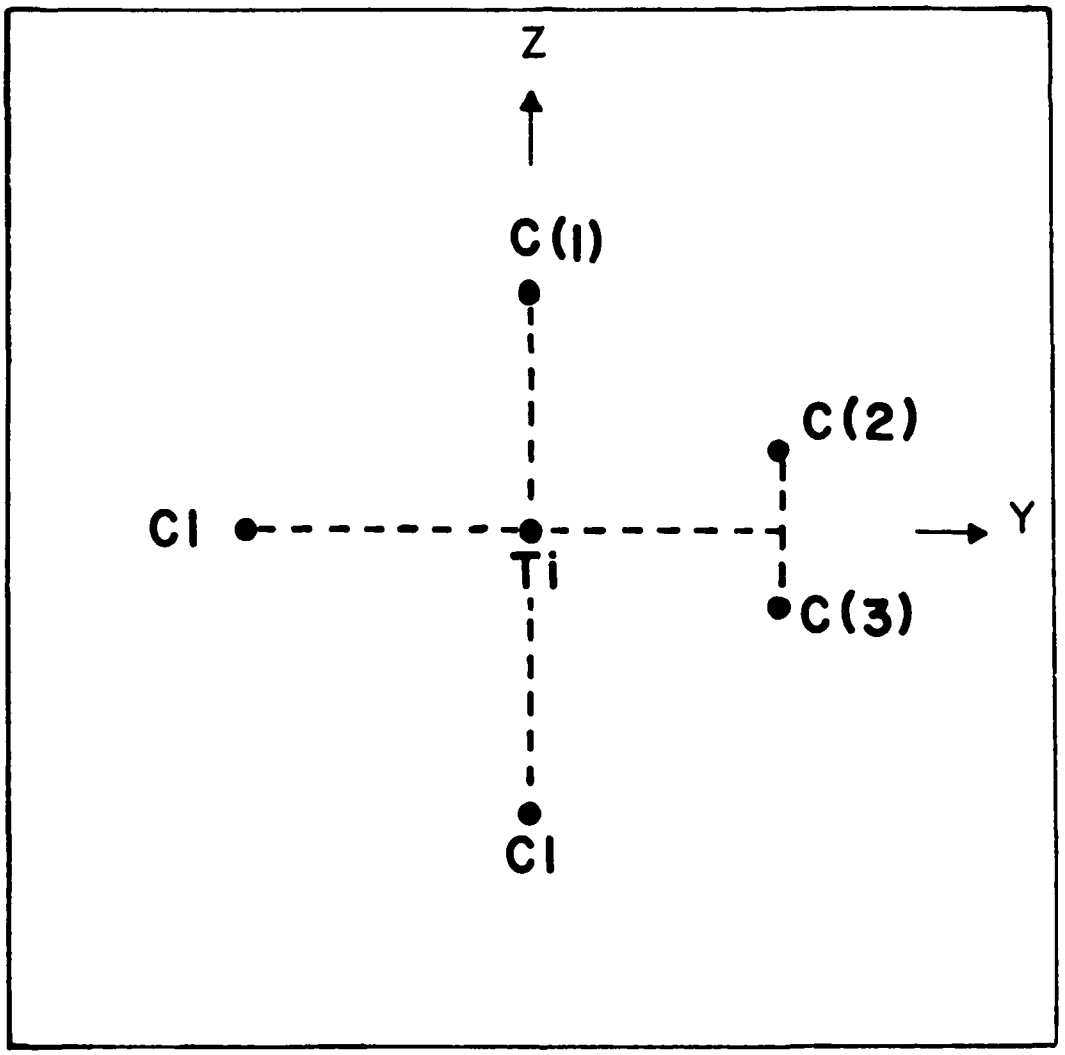
Z
C(1)
C(2)
Cl
Y
Ti
C(3)
Cl

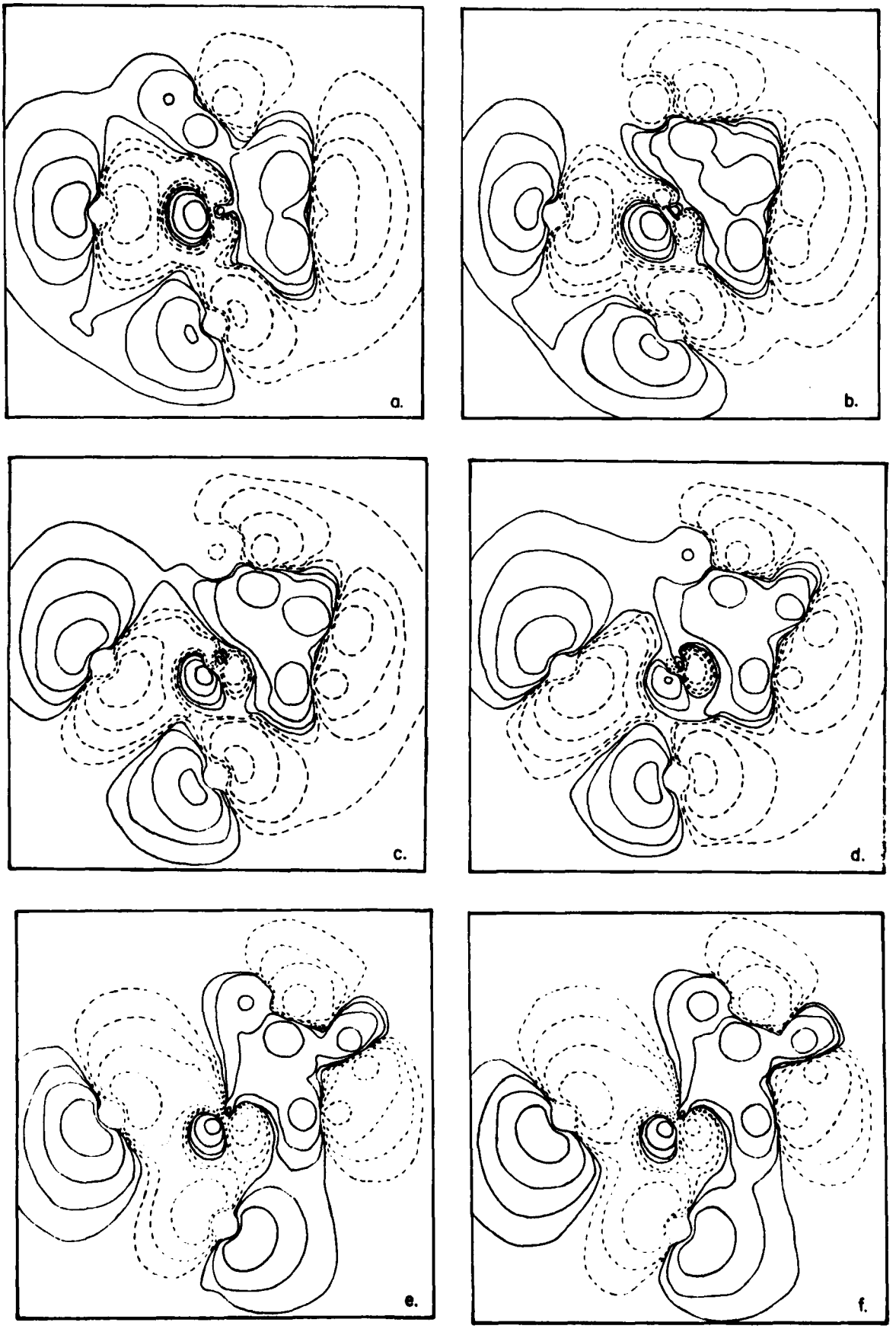
a.
b.
c.
d.
e.
f.

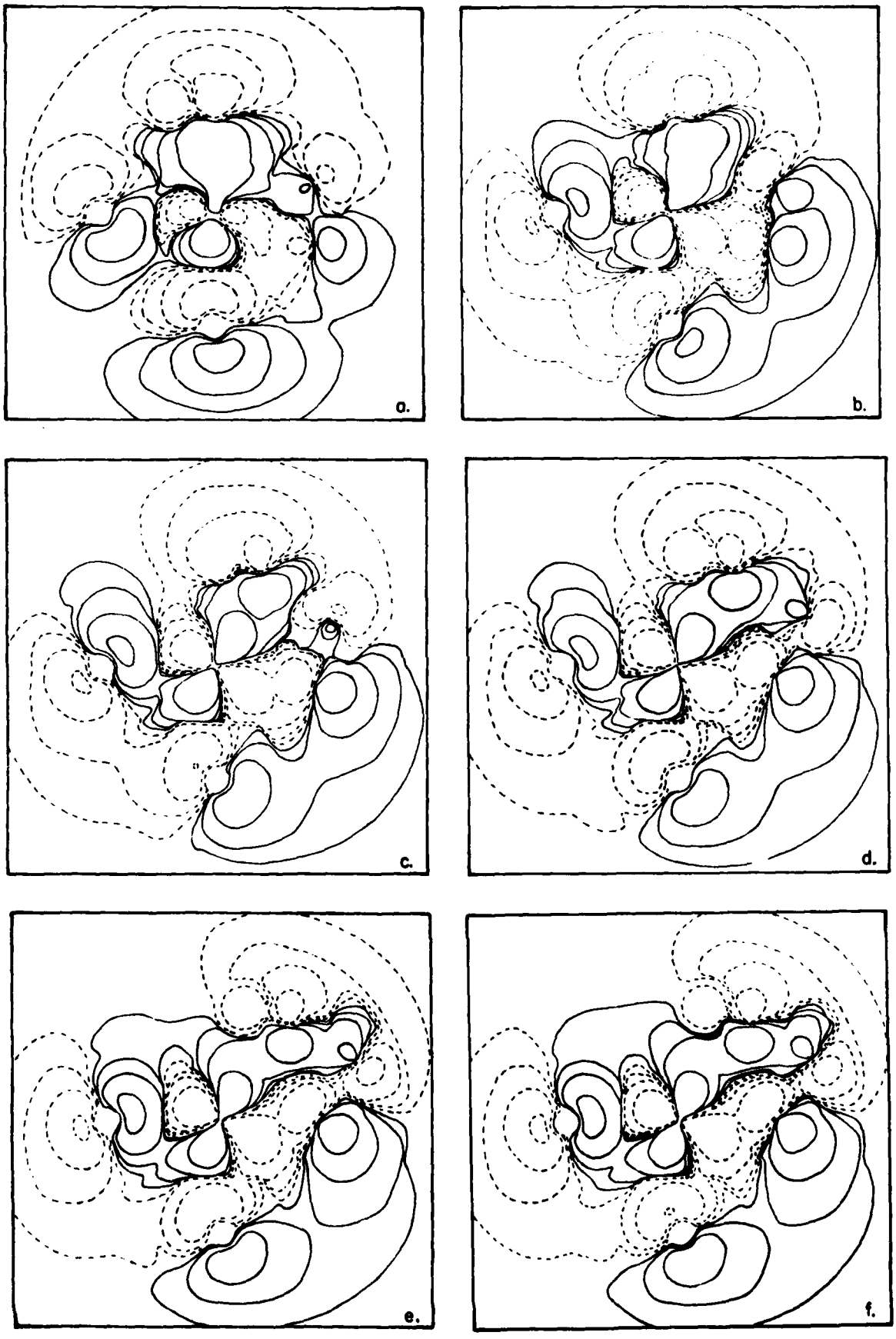
a.
b.
c.
d.
e.
f.

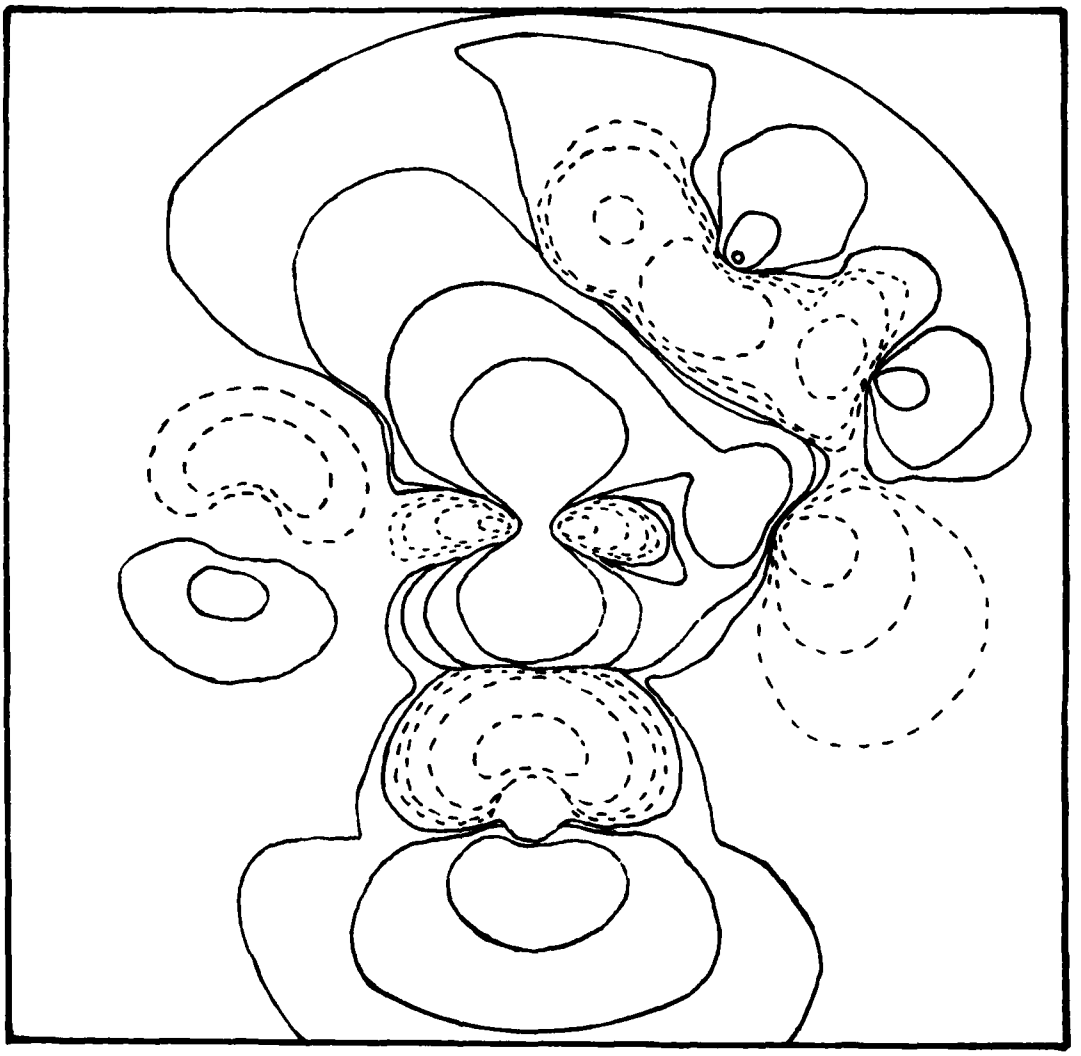

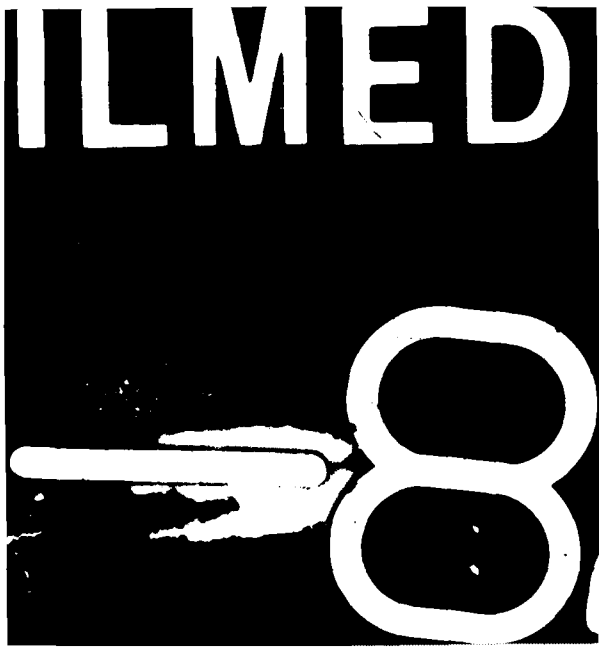
ILMED
8